Journal of Alloys and Compounds 509 (2011) 6106–6112

Contents lists available at ScienceDirect

Journal of Alloys and Compounds

journal homepage: www.elsevier.com/locate/jallcom

Microstructural mapping in closed die forging process of superalloy Nimonic 80a valve head

Zhu Yuanzhi [a,b,*], Yin Zhimin [c], Xu Jiangpin [b]

[a] Key Laboratory for Ferrous Metallurgy and Resources Utilization of Ministry of Education, Wuhan University of Science and Technology, Wuhan 430081, China
[b] School of Materials and Metallurgy, Wuhan University of Science & Technology, Wuhan 430081,China
[c] School of material science and engineering, Central south university, Changsha 410083,China

ARTICLE INFO

Article history:
Received 8 December 2010
Received in revised form 3 March 2011
Accepted 6 March 2011
Available online 11 March 2011

Keywords:
Nimonic 80a
Upsetting and closed die forging
Microstructral map
Modeling

ABSTRACT

Optical microscopy, XRD, TEM and FEM were used to study the microstructral map in the alloy in the upsetting and closed die forging processes. The maps of hardness, grain size, dislocation and the secondary phase γ′ in the upset and closed die forged nimonic 80a alloy valve head were investigated. It is found that the metals flowed from the asymmetric central axis outwards in the upsetting and forging process. The flowing model of metals together with the thermal field led to a heterogeneous distribution of grain size, dislocation configuration and the secondary phase γ′. It is also necessary to mention that the largest grain size, the lowest density of dislocation and secondary γ′ phase only occurred in the transitional region between the valve head and valve stem, which may weaken the strength in this region.

© 2011 Elsevier B.V. All rights reserved.

1. Introduction

Nimonic 80a is a superalloy widely used in aerospace and other industries because of its high strength and strong resistance to corrosions [1–4]. It is also attractive to engineers to fabricate exhausting valve head for high power engines [5,6]. Besides the above stated advantages, the alloy has its weakness, such as low wearing resistance. To overcome this shortcoming, compound exhausting valve was usually fabricated. Nimonic 80a alloy was often used to make valve head, while a martensite stainless steel or other high wear resistant materials were used to make the valve stem [7]. If the engine is like the "heart" of automobiles or aircrafts etc., the valve is just like a heart valve. The failure of engine valves can lead to the failure of the whole engine. Valves, especially the exhausting valve, are frequently operated at conditions of corrosion and creep at temperatures as high as 500–800 °C, or even higher. Valves often failed due to fracture, with deformation in the valve head [8,9]. Thus, valve heads have to be carefully fabricated. The quality of valve head made from Nimonic 80a superalloy mainly depends on its fabrication processes. The microstructure of valve head in forging processes is a decisive factor to its later properties in applications. Jeong studied the recrystallization of the alloy in closed die forging processes [10]. Actually, more detailed studies on secondary phase precipitation, dislocation configuration and deformation mechanism are still necessary to ensure the reliabilities of the valve head. Here, a microstructural map including these details matching strain field in the closed forging process is provided, which may offer a new insight for engineers in this field to adjust forging process parameters of the alloy to ensure a high quality of the valve head.

2. Experimental

Valve heads were prepared in two processes: upsetting and closed die forging.

Nimonic 80a alloy bar in a diameter of φ 16 mm was heated to 1100 °C and upset into an ellipsoidal workpiece. After that, the workpiece was forged into a valve head in a closed die as quickly as possible, as shown in Fig. 1.

The valve head was cut apart along the asymmetric central axis with a numerical controlled linear cutting machine. Hardness measurement was performed both along the asymmetric central axis and on the bottom surface vertical to the asymmetric central axis. Optical microscopy observations were performed at different locations along the longitude section across the asymmetric central axis. Several pieces of samples were also cut down every 1 mm vertical to the asymmetric central axis. These sections were polished for XRD analysis, which was performed on a Rigaka X-ray diffractometer with a scanning rate of 0.1 °/min. A $Cu_{k\alpha}$ source and a voltage of 2 kW were used for the analyses.

After XRD measurement, the sections were mechanically polished to a thickness of 0.1 mm and then were jet-polished with a solution of 5% $HClO_4$ in ethanol with a voltage of 15 V. The prepared foils were used for TEM observation. TEM observation was performed on a H800 transmission electron microscope.

* Corresponding author at: Key Laboratory for Ferrous Metallurgy and Resources Utilization of Ministry of Education, Wuhan University of Science and Technology, Wuhan 430081, China.
E-mail address: tozyz1@163.com (Y.Z Zhu).

0925-8388/$ – see front matter © 2011 Elsevier B.V. All rights reserved.
doi:10.1016/j.jallcom.2011.03.038

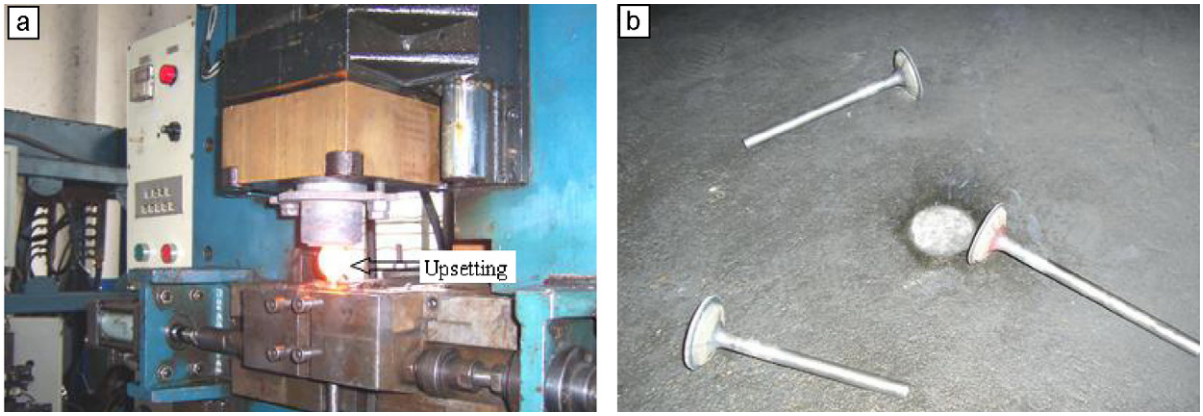

Fig. 1. Upsetting and closed die forging of the valve head. (a) Upsetting of the Nimonic 80a alloy, (b) Closed die forged valve head.

3. Results and discussions

3.1. Hardness mapping and optical microscopy of the closed-die forged valve head

Hardness map of the forged valve head was given in Fig. 2. It shows that the hardness decreases from the bottom surface to the valve stem along the asymmetric central axis. The bottom surface has the highest hardness of 37.5HRC, while the stem has the lowest hardness of 30HRC. There is a sharp change in hardness in the transitional region (in 20–25 mm) from the bottom surface of the valve head to the stem, which may be attributed to different work hardening effects at different locations for heterogeneous deformation in the valve head part. In the stem near the valve head, there is no deformation in this region. And at the same time, heat from the valve head enhances the temperature in the transitional region (in 20–25 mm), leading to softening in this transitional region by recrystallization and recovery. The changes in hardness in the transitional region are due to a gratitude thermal field here. However, in the valve head, metals flow strongly in the forging deformation process, in which working hardening occurs and hardness increases. In the fabrication process of the valve head, the duration time was

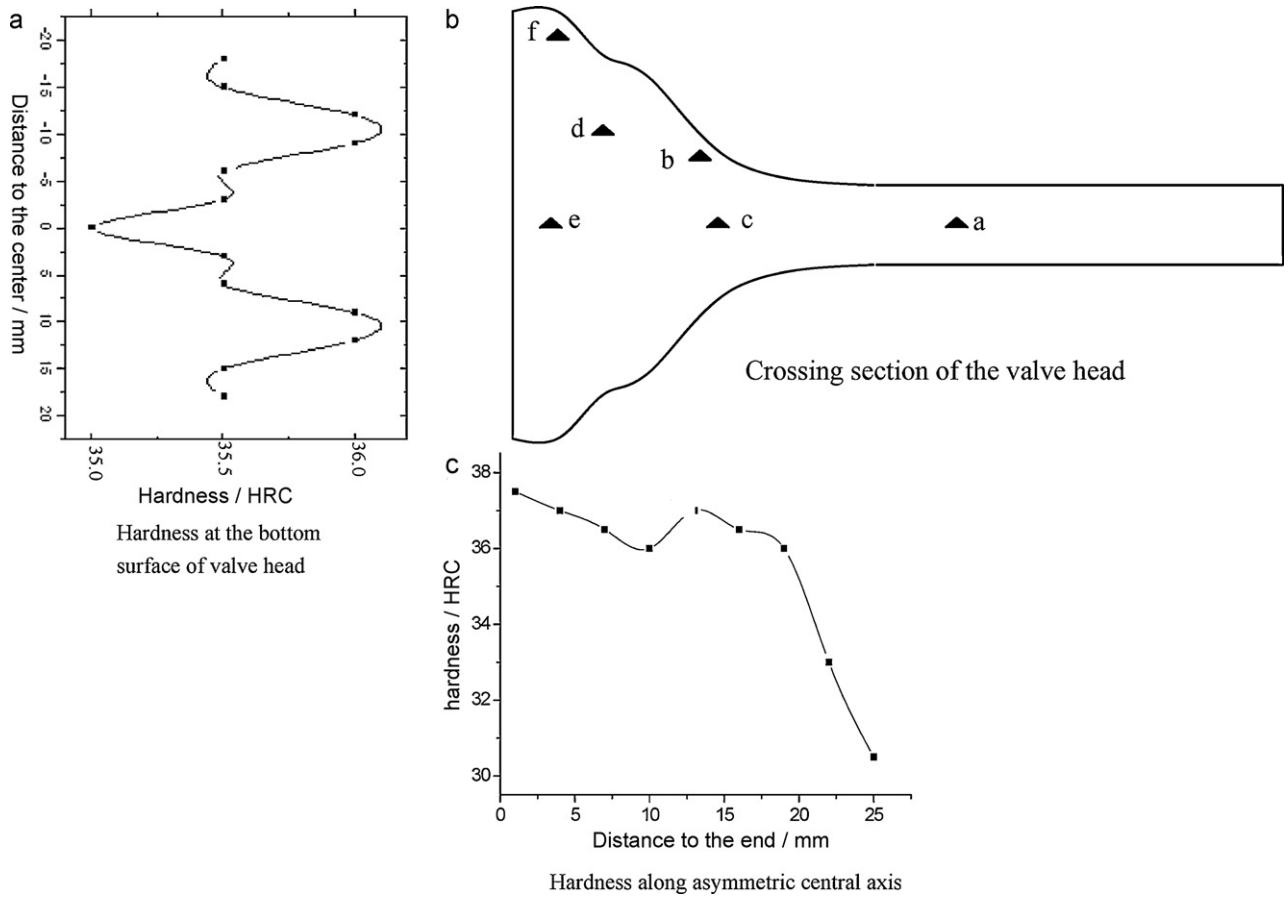

Fig. 2. Hardness map of the close die forged valve head.

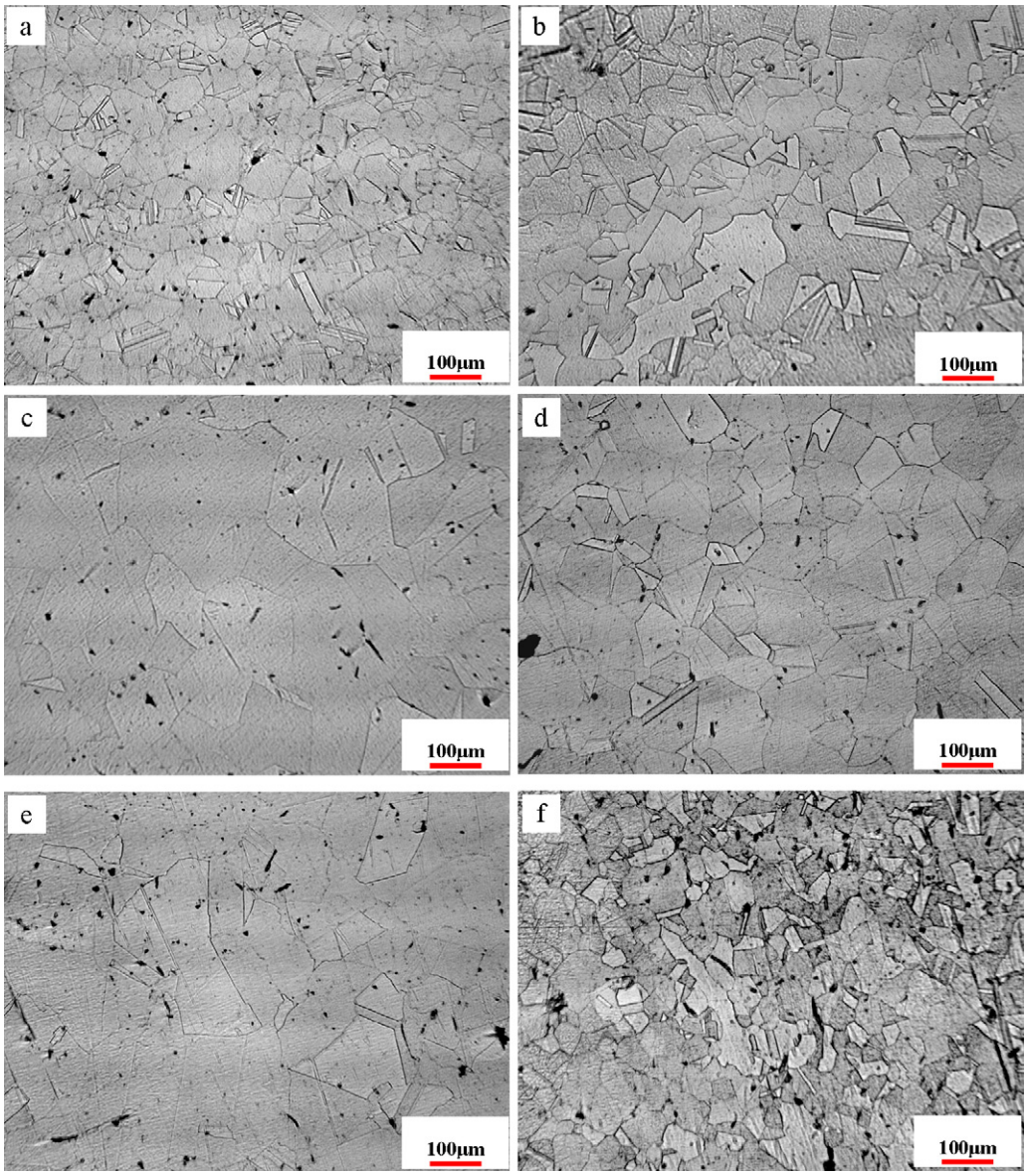

Fig. 3. Optical micrograph map of the valve head closed die forged. (a)–(f) correspondent to points (a)–(f) in Fig. 2, respectively.

about one minute and the effect of work hardening was greater than that of softening from recovery and recrystallization of the alloy. Therefore, the hardness increases from the stem to the bottom surface for different strain and thermal effect. The bottom surface has the highest hardness value because the metals at this location had undergone a large deformation in the upsetting and forging processes and then cooled at a high cooling rate. On the bottom surface of the valve head, the hardness value varies from 35 to 36HRC. The shape of the hardness value curve is like "w". It has the lowest hardness value of 35HRC at the central point on the bottom surface, while it has the highest hardness at the points of 1/4 diameter from the central of the bottom surface. This kind of difference in hardness mainly depends on the different extent of deformation at different locations.

The optical microscopy of the valve head is illustrated in Fig. 3. It shows that the edge of the bottom surface of the valve head has the finest but most heterogeneous microstructures. Maybe, metals at this location were deformed with very large strain. However, the plastic flow of the metals at this location is heterogeneous, resulting in a heterogeneous microstructure. The grain sizes in point "c" and "e" are large. The maximum grain size in these regions is of several millimeters, implying an occurrence of recrystalliztion of the alloy in the regions. Both points are just located on the asymmetric central axis, where the cooling rate may be lowest in the upsetting and forging processes. Long duration at high temperature may have caused a coarsened microstructure. It is also found that there are more twin crystals in the alloy in locations undergone a larger strain than in those undergone a lower one.

3.2. TEM micrograph of the alloy after upsetting and forging

The TEM micrographs of the upset and forged valve head are given in Fig. 4. High angle grain boundaries can be observed in the transitional region between the valve head and the valve stem (see Fig. 4e–f). In this region, the densities of both dislocations and the secondary phase γ' are very low. Moreover, the visible γ' phase is coarsened. The characteristics in this region is in coincidence with the hardness map of the valve head. Static recrystalliztion and grain

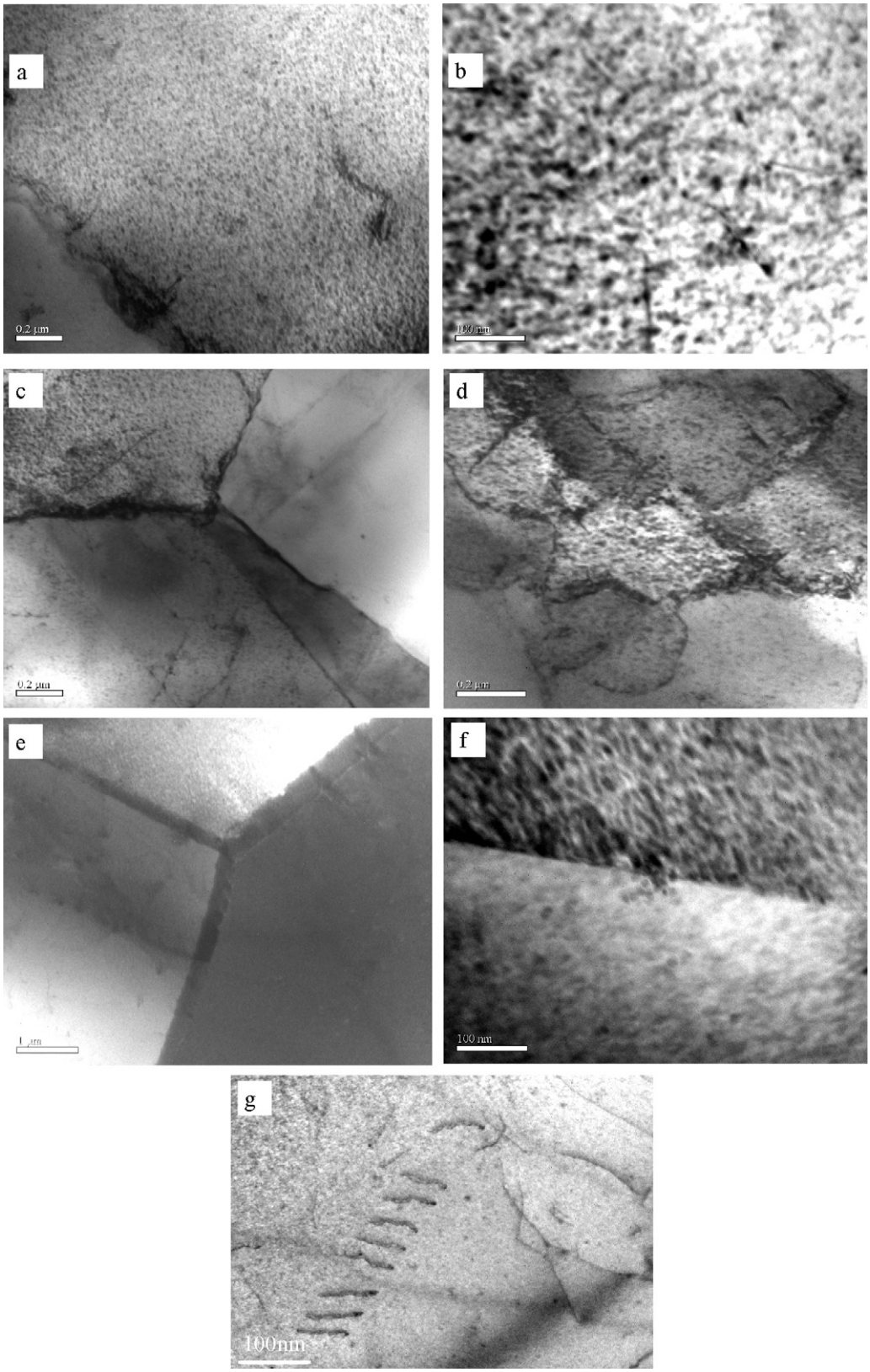

Fig. 4. TEM micrograph of the alloy after upsetting and closed die forging. (a) and (b) Point e in Fig. 2. (c) and (d) Point f in Fig. 2 (e) and (f) Point c in Fig. 2. (g) Point b in Fig. 2.

growth mainly has occurred in the region. Microstructures in the bottom surface of the valve head are completely different from this transitional region. A recovery microstructure is visible in the centre of the bottom surface. The density of γ′ phase is high and its size is larger than that in other regions. At the edge of the bottom surface, a typical cellular microstructure can be seen. A rather high dislocation density is present in this region. γ′ phase cannot be seen very clearly in the region, probably due to its too small size.

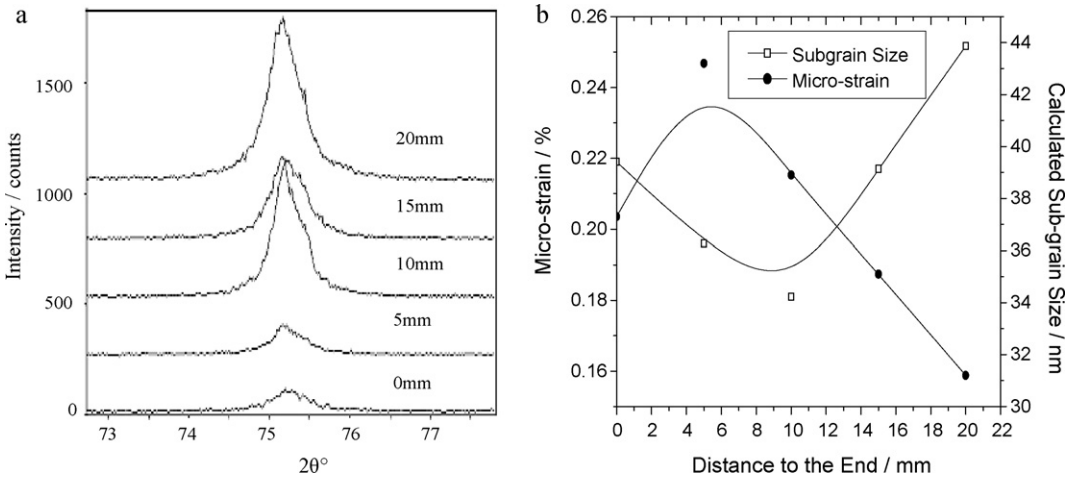

Fig. 5. Microstrain and subgrain size in the alloy in a range from 0 to 20 mm along the central asymmetric line of the valve head. (a) XRD pattern, (b) Microstrain and subgrain size.

The microstructual differences between the transitional region and the bottom surface would result from the much larger deformation in the bottom surface than in the transitional region.

3.3. Microstrain and subgrain size of the valve head along the asymmetric central axis

Samples were cut down every 1 mm along the asymmetric central axis by a numerically controlled linear cutting machine. Then, they were polished on both sides. Microstrain and subgrain size were measured by an attached XRD system with analysis software. The microstrain and subgrain size are illustrated in Fig. 5.

It shows that there is a peak in microstrain at the location about 5 mm away from the bottom surface (end) of the valve head. The smallest subgrain size occurs at the location about 10 mm from the bottom surface of the valve head. The appearance of the maximum microstrain and smallest subgrain size at different locations in the valve head is probably caused by the heterogeneousness of the both thermal field and strain field, and also the orientation of the grains. Microstrains are just related to d-spacings in the alloy, while subgrain size depends on coherent scattering domain sizes.

The largest subgrain size occurs at the transitional region from the valve head to the valve stem, which coincides with the TEM observation.

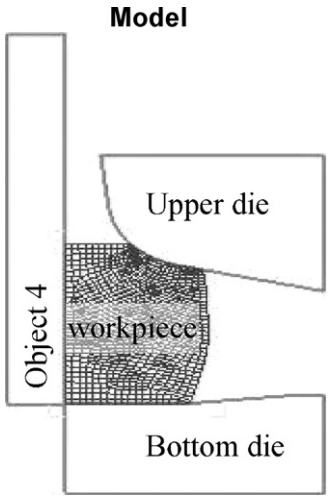

Fig. 6. A geometric model of closed die forging for FEM calculation.

3.4. Finite element modeling of the forging process

A better understanding of the microstructure map in the forged valve head can be achieved more precisely by modeling the forging

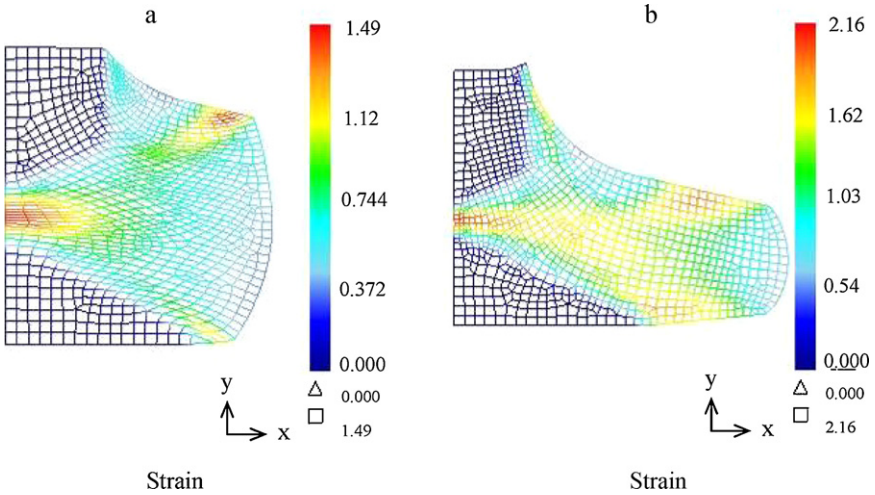

Fig. 7. Strain field at different time in the forging process (a) 1.05 s (b) 1.5 s.

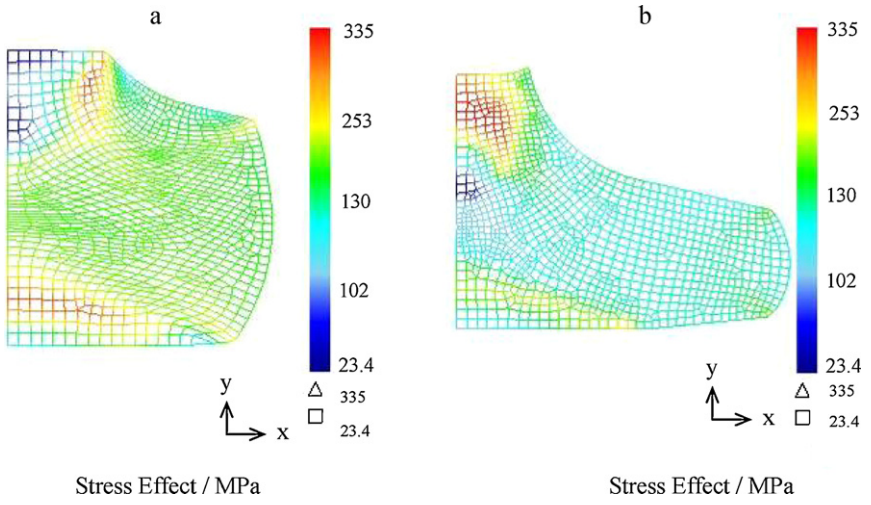

Fig. 8. Stress field at different time in the forging process (a) 1.05 s (b) 1.5 s.

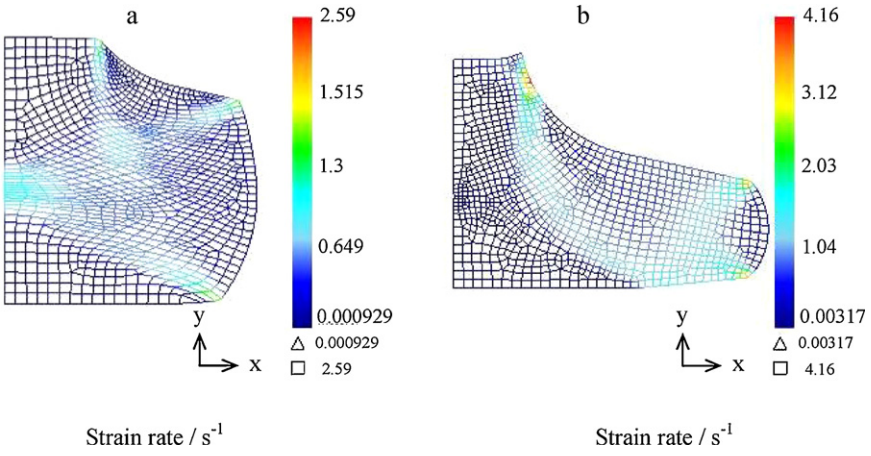

Fig. 9. Strain rate at different forging time (a) 1.05 s (b) 1.5 s.

processes. The geometry of the valve head is axisymmetric. Thus, the geometric model can be simplified as a 2D problem, which is illustrated in Fig. 6. The constitutive relations and the correspondent parameters of the Nimonic 80a workpiece were reported in reference [11,12]. Two preconditions are assumed: (1) no heat flow between object 4 and the workpiece; (2) the thermal conductivity between the upper die and the workpiece is the same as that between the bottom die and the workpiece. The bottom die and object 4 are both stationary in the whole forging processes. A commercial FEM code of deform 2D has been used in this simulation.

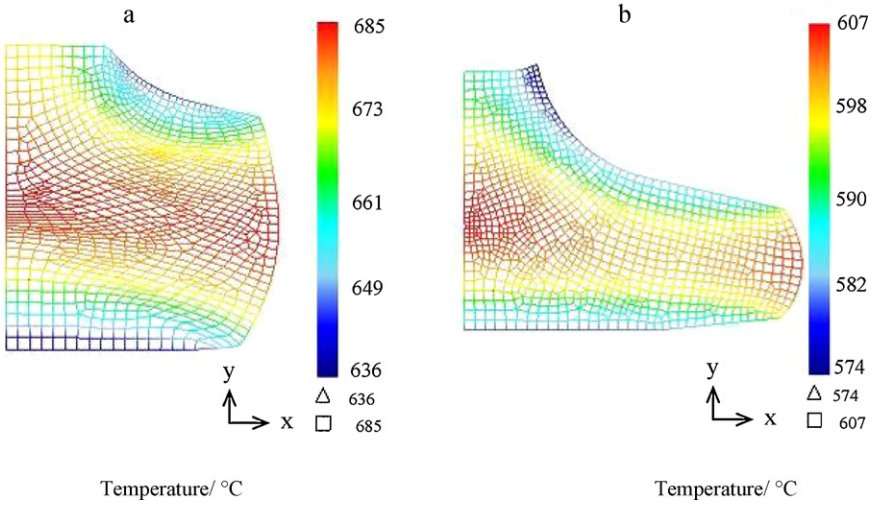

Fig. 10. Thermal field at different forging time (a) 1.05 s (b) 1.5 s.

The modeling results are given in Figs. 7–10. It shows that it has the highest strain in the centre of the workpiece. The deformation propagates from the centre down to the bottom surface and outwards to the outside edge of the valve head in the forging process.

Stress field in the workpiece in the forging process is given in Fig. 8. It shows that the strain field does not coincide with the stress field. The maximum stresses occurs at the transitional regions between the large strain region (region in yellow or green) and small strain region (region in blue). This heterogeneous stress field may lead to the propagation of strain from the deformed regions to undeformed regions, which is helpful to a smooth occurrence of the forging process.

The calculated velocity field is shown in Fig. 9. It shows that the velocity field propagates gradually from the centre outwards the edge of the valve head. The velocity field may be influenced by the strain field, which influences the work hardening of the alloy, and the stress field which directly influences the "driving force" of the motion regional metals.

Thermal field has been illustrated in Fig. 10. Here thermal field mainly depends on the geometry of the workpiece. The central of the workpiece usually has a higher temperature than that in surface regions Thermal field, strain field and stress field interact with each other.

4. Conclusions

The maps of hardness, grain size, dislocation and the secondary phase γ' in the upset and closed die forged Nimonic 80a alloy valve head were investigated and measured. Finite element modeling was used to trace the history of thermal field, strain field and the tress field. It is found that the metals flowed from the asymmetric central axis outwards in the upsetting and forging process. The flowing model of metals together with thermal field led to a heterogeneous distribution of grain size, dislocation configuration and the secondary phase γ'. It is also necessary to mention that the largest grain size, the lowest density of dislocation and secondary γ' phase only occurred in the transitional region between the valve head and valve stem, which may lead to fracture in its later applications.

Acknowledgement

This work is supported by The National Natural Science Foundation of China (no. 50874083, 51074117), the Foundation for Distinguished Young Scientists of Hubei Province of China (no. 2009CDA044), the Foundation of Hu'bei Educational Committee no. Q20091110 and the Foundation of Hu'nan Science and technology (no: 2009WK3045).

References

[1] J. Lyyränen, J. Jokiniemi, E.I. Kauppinen, Fuel Process. 86 (4) (2005) 353–373.
[2] D. Clark, M.R. Bache, M.T. Whittaker, J. Mater. Process. Technol. 203 (1–3) (2008) 439–448.
[3] W. Betteridge, Mater. Sci. Technol. 3 (9) (1987) 682–694.
[4] T. Moriyama, Y. Izaki, K. Umeda, R. Oka, Y. Nishioka, T. Tanaka, Mater. Sci. Technol. 10 (11) (1994) 993–1001 (9).
[5] K.H. Mayer, H. Konig, Damage Assessment of Service Stressed Nimonic 80A Steam Turbine Bolts, Institute of Materials, UK, 1995, 1995 pp. 343–355.
[6] M. Izaki, T. Moriyama, M. Abe, T. Okuda, Kobe Res. Develop. 44 (2) (1994) 50–54.
[7] Y.Z. Zhu, Z.M. Yin, D.M. LIANG, J.C. Li, Z.D. Xiang, ISIJ Int. 50 (11) (2010) 1666–1670.
[8] T.R. Meyer, R.A. White, International Congress & Exposition, February 1998, Detroit, MI, USA, Session: New Diesel Engines & Components.
[9] Y.S. Wang, S. Narasimhan, J.M. Larson, J.E. Larson, G.C. Barber, Wear 201 (1-2) (1996) 15–25.
[10] H.S. Jeong, J.R. Cho, H.C. Park, J. Mater. Process Technol. 162–163 (2005) 504–511.
[11] D.K. Kim, D.Y. Kim, S.H. Ryu, J. Mater. Process. 113 (1-3) (2001) 148–152.
[12] H. Teng, Z.M. Yin, Y.Z. Zhu, K.C. Zhou, Z.Y. Li, Acta metall. Sinica. 42 (6) (2006) 629–634.